Available online at www.sciencedirect.com
ScienceDirect
Acta Materialia 59 (2011) 4404–4415
Acta MATERIALIA
www.elsevier.com/locate/actamat

Equilibrium viscosity, enthalpy recovery and free volume relaxation in a $Zr_{44}Ti_{11}Ni_{10}Cu_{10}Be_{25}$ bulk metallic glass

Zach Evenson *, Ralf Busch

Saarland University, Chair for Metallic Materials, Campus C6.3, D-66123 Saarbrücken, Germany

Received 25 October 2010; received in revised form 23 March 2011; accepted 24 March 2011
Available online 15 April 2011

Abstract

We report on the free volume of a $Zr_{44}Ti_{11}Ni_{10}Cu_{10}Be_{25}$ bulk metallic glass (BMG) in terms of its experimentally determined volumetric relaxation, enthalpy recovery and equilibrium viscosity below the glass transition temperature T_g. The results obtained present a very consistent picture of structural relaxation as analyzed by calorimetric and volumetric methods. At annealing temperatures below T_g a linear correlation is found between the experimentally determined enthalpy of recovery and free volume reduction, giving a constant value for the formation enthalpy of the free volume in the glass. The free volume in the equilibrium liquid is calculated from viscosity measurements carried out below T_g. These data are described using the Cohen–Turnbull and Cohen–Grest models of the free volume. Additionally, an interpretation of the free volume based on the Adam–Gibbs equilibrium viscosity model is proposed. Analysis of the free volume and enthalpy functions of the equilibrium liquid reveals a temperature-dependent formation enthalpy for the free volume that varies from ~1 eV at the melting point to ~2 eV near the glass transition. Finally, we analyze the melt viscosity of the $Zr_{41.2}Ti_{13.8}Cu_{12.5}Ni_{10.0}Be_{22.5}$ BMG and find that the Adam–Gibbs model gives the best prediction of the free volume at high temperatures.

Keywords: Bulk metallic glasses; Free volume; Viscosity; Structural relaxation; Enthalpy recovery

1. Introduction

The formation of a glass during undercooling from a liquid is associated with the "freezing in" of a certain amount of excess free volume as the liquid falls out of equilibrium at the glass transition temperature T_g. A good conceptualization of the free volume of a melt as the glass transition is approached is given by understanding the kinetic slow down in terms of viscosity. The change in viscosity with temperature reflects an intrinsic property of glass-forming liquids known as fragility. Glass formers that show very little change in their equilibrium viscosity as T_g is approached are defined as being kinetically "strong", i.e. they exhibit an Arrhenius dependence of the viscosity on temperature, where substances whose equilibrium viscosities vary much more with temperature are classified as "fragile" [1,2]. The temperature dependence of the equilibrium viscosity can be described by the empirical Vogel–Fulcher–Tammann (VFT) equations [3–5]

$$\eta = \eta_0 \exp\left(\frac{D^* T_0}{T - T_0}\right) \tag{1}$$

The parameter D^* is the kinetic fragility of the material; the most fragile glass formers have a fragility of around 2, whereas the strongest are of the order of 100. The VFT temperature T_0 is the temperature at which the barriers with respect to flow approach infinity [2]. The pre-exponential factor η_0 is fixed at a value of 4×10^{-5} Pa s, according to the relation $\eta_0 = h/v_m$, where h is the Planck constant and v_m is the atomic volume [6].

* Corresponding author. Tel.: +49 0 681 302 2248; fax: +49 0 681 302 4385.
E-mail address: z.evenson@mx.uni-saarland.de (Z. Evenson).

1359-6454/$36.00 © 2011 Acta Materialia Inc. Published by Elsevier Ltd. All rights reserved.
doi:10.1016/j.actamat.2011.03.064

A phenomenological model of the equilibrium viscosity of glass-forming substances was formulated in terms of the free volume by Doolittle [7]

$$\eta = \eta_0 \exp\left(\frac{bv_m}{v_f}\right) \tag{2}$$

where v_f is the average free volume per atom of the equilibrium liquid and the parameter b is a material-specific constant of order unity. The term bv_m represents the critical volume necessary for viscous flow. In the present study we define the free volume as in Doolittle [7], i.e. it is the difference between the specific volume and occupied volume at a given temperature. The model of Cohen and Turnbull assumes a linear relation between the free volume and temperature [8]

$$v_f = v_m \alpha_f (T - T_0) \tag{3}$$

where α_f can be approximated by the difference between the volumetric thermal expansion coefficients of the liquid and the glass, $\alpha_f = \alpha_{liq} - \alpha_{glass}$ [9,10]. In this model of the free volume viscous flow occurs as a result of random density fluctuations that allow diffusion of individual atoms without change to the local free energy [11]. In other words, viscous flow is attributed not to energy barriers, but rather to the redistribution of free volume. Assuming that T_0 is the temperature at which the free volume of the equilibrium liquid vanishes and viscous flow is no longer be possible, it becomes immediately apparent that by substituting Eq. (3) for the free volume in Eq. (2) the VFT equation (Eq. (1)) is recovered with the relation $\alpha_f = b/(D^* T_0)$. In an extended model of the free volume by Cohen and Grest [12] the metastable equilibrium liquid is partitioned into cells, whose free energy is a function of the cell volume. Each cell then behaves either like a liquid, capable of diffusive motion, or like a solid, capable of only oscillatory motion. Taking the Cohen and Grest expression for the free volume

$$v_f = \frac{k}{2\varsigma_0}\left(T - T_q + \sqrt{(T - T_q)^2 + \frac{4v_a\varsigma_0}{k}T}\right) \tag{4}$$

and inserting it into Eq. (2) yields the parameters $bv_m\varsigma_0/k$, T_q and $4v_a\varsigma_0/k$. In this newer model of the free volume v_f does not vanish at T_0. Instead, the free volume remains greater than 0 at all temperatures and only vanishes when $T = 0$. The viscosity, therefore, would not diverge and remain well defined for all temperatures.

Another phenomenological model of the equilibrium viscosity, based on the thermodynamic functions of the undercooled liquid, is the Adam–Gibbs entropy model for viscous flow [13]

$$\eta = \eta_0 \exp\left(\frac{C}{T \cdot S_c(T)}\right) \tag{5}$$

where $S_c(T)$ is the configurational part of the entropy of the equilibrium liquid and the parameter C can be understood as a free energy barrier per particle for cooperative rearrangements. The function $S_c(T)$ can be calculated from the experimentally determined thermodynamic functions of the material as

$$S_c(T) = S_c(T_m^*) - \int_T^{T_m^*} \frac{\Delta C_p^l - x(T')}{T'} dT' \tag{6}$$

leaving the parameters C and $S_c(T_m^*)$ to be determined though fitting of the experimental data, where T_m^* is a scaling parameter chosen as the temperature for which the viscosity of the melt has a value of 1 Pa s [14]. It is assumed here that the vibrational contribution to the entropy for both the undercooled melt and the crystal are similar. Hence, the configurational part of the entropy decreases during undercooling at the same rate as the entropy difference between the liquid and the crystal, where ΔC_p^{l-x} is the difference in the specific heat capacities of the liquid and the crystal. By comparing Eqs. (2) and (5) it is now possible to express the relative free volume of the equilibrium liquid in terms of its configurational entropy as

$$\frac{v_f}{v_m} = \frac{b \cdot T \cdot S_c(T)}{C} \tag{7}$$

The free volume has recently been investigated in various bulk metallic glass (BMG) forming systems through, for example, direct density measurements [15–18], viscosity studies [9,19–22] and positron annihilation lifetime measurements [23]. Van den Beukel and Sietsma proposed a method for quantifying the free volume in terms of enthalpy as measured using differential scanning calorimetry (DSC) [24]. This method has since been employed by several researchers, using enthalpy relaxation to examine the free volume of BMGs at temperatures below the glass transition [16,18,25–31].

In the present study we investigate the free volume of a $Zr_{44}Ti_{11}Ni_{10}Cu_{10}Be_{25}$ (Vitreloy 1b™) BMG alloy at temperatures below T_g using independent measurements of enthalpy recovery, length relaxation and equilibrium viscosity. The isothermal relaxation in length is used to directly determine the reduction in the excess free volume present in the glassy sample. Equilibrium viscosity data taken in the vicinity of T_g are used as a basis for constructing free volume curves of the equilibrium liquid using the different models of the free volume proposed in Eqs. (3), (4), and (7). We compare the amount of structural relaxation occurring in each of the three measured quantities and relate these within the framework of the free volume model. Finally, we revisit the case of free volume and viscous flow in the $Zr_{41.2}Ti_{13.8}Cu_{12.5}Ni_{10.0}Be_{22.5}$ (Vitreloy 1™) alloy as reported in Masuhr et al. [9] and use recent high temperature viscosity data to test the efficacy of each of the proposed free volume models in the liquid state.

2. Experimental methods

Fully amorphous rods of $Zr_{44}Ti_{11}Ni_{10}Cu_{10}Be_{25}$ were supplied by Liquidmetal© Technologies. Calorimetric

experiments were carried out with a power compensated Perkin–Elmer Diamond DSC in high purity aluminum pans under a constant flow of high purity argon gas. The DSC was calibrated for each heating rate according to the melting transitions of indium and zinc, as well as the β–α phase transformation of K_2SO_4. The dilatometric measurements were carried out in a Netzsch thermal mechanical analyzer (TMA 402) calibrated for heating rates of 0.025, 0.416 and 0.833 K s^{-1} according to the melting standards of indium and zinc. During the experiments the TMA chamber was purged with high purity argon gas at a rate of 50 ml min^{-1}. To investigate the enthalpy and free volume changes on a long time scale the specimens were first equilibrated in the supercooled liquid region at a temperature of 700 K and immediately cooled down to room temperature at a rate of 0.416 K s^{-1}. This ensured the same enthalpic state for each of the amorphous samples.

Enthalpy relaxation was carried out during DSC by first heating each sample, with masses ranging from 80 to 100 mg, to the desired annealing temperature before the onset of the calorimetric glass transition, at a rate of 0.416 K s^{-1}, and then holding isothermally for a certain amount of time. At each annealing temperature the samples were held for various times. The maximum annealing time at each temperature was chosen to be long enough to completely relax the samples (see, for example, Launey et al. [29]) and ensure relaxation into the equilibrium liquid while avoiding the crystallization events measured isothermally in Waniuk et al. [32]. After completion of the anneal the samples were first cooled to room temperature at a rate of 0.416 K s^{-1} and then subsequently heated at the same rate through the glass transition, where enthalpy recovery was measured, and past the crystallization event to a temperature of 853 K.

Volumetric measurements of the relaxation below T_g were carried out in the TMA (dilatometer mode) using a vertical, fused silica loading probe. Rectangular samples with dimensions of approximately $2 \times 2 \times 8$ mm were cut from the rods and used for the dilatometric measurements. The glassy samples were heated at a rate of 0.416 K s^{-1} to the desired temperatures and then held isothermally and the length relaxation directly measured. The load on the sample surface was applied by a spring-loaded linear variable differential transformer and was calculated to be 0.20 ± 0.04 mN.

Additionally, beams with rectangular cross-sections between 0.2 and 1.0 mm^2 and lengths of approximately 13 mm were cut from the samples and a three-point beam bending method was used to measure the viscosity in the vicinity of the glass transition. A beam, supported at each end by sharp edges, is subjected in the center to a constant force provided by a fused silica loading probe with a wedge-shaped head and the corresponding deflection of the beam is measured. Using this technique viscosities ranging from 10^7 to 10^{14} Pa s can be determined with the equation [33]

$$\eta = -\frac{gL^3}{144 I_c v}\left[M + \frac{\rho A L}{1.6}\right] \tag{8}$$

where g is the gravitational constant (m s^{-2}), I_c is the cross-section moment of inertia (m^4), v is the mid-point deflection rate (m s^{-1}), M is the applied load (kg), ρ is the density of the glass (kg m^{-3}), A is the cross-sectional area (m^2) and L is the support span (1.196×10^{-2} m for the apparatus). The applied load was kept constant at 0.01 kg while the cross-section of the beams varied, depending on the expected viscosity at a given temperature.

The absolute specific heat capacity of this alloy in the glassy supercooled liquid and crystalline states was determined using the DSC step method outlined in Gallino et al. [34]. Additionally, a Netzsch STA 449 C differential thermal analyzer (DTA) was used to detect the melting point and heat of fusion of the sample enclosed in a graphite crucible with high purity argon as the purging gas.

3. Results

Fig. 1 shows the DSC and DTA traces of a glassy sample of $Zr_{44}Ti_{11}Ni_{10}Cu_{10}Be_{25}$ scanned at heating rates q_H of 0.416 and 0.50 K s^{-1}, respectively. The onset temperature of the glass transition T_g^{onset} and the beginning of the crystallization event T_x occur in DSC for this heating rate at 620 and 774 K, respectively. The melting temperature T_{eut} in the DTA was 921 K and the liquidus temperature T_{liq} was 1102 K, at which the sample was completely molten.

In Fig. 2 the enthalpy recovery curves of the completely annealed samples (dotted lines) are shown after heating at $q_H = 0.416$ K s^{-1} across the glass transition. The recovery curves are shown alongside a scan of the unrelaxed sample (solid line), i.e. a sample that was heated at the same rate q_H as an immediately preceding cooling q_C from the supercooled liquid region. It was previously established that if the convention $q_H = q_C$ holds then the measured onset temperature of the glass transition on heating T_g^{onset} approxi-

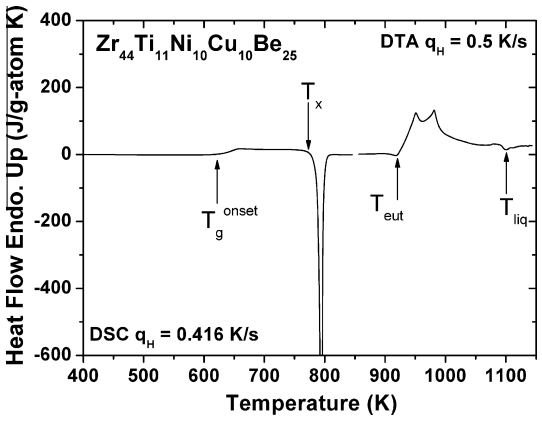

Fig. 1. DSC and DTA thermograms of an as-cast sample of the $Zr_{44}Ti_{11}Ni_{10}Cu_{10}Be_{25}$ BMG with heating rates q_H of 0.416 and 0.50 K s^{-1}, respectively. T_g^{onset} (620 K), T_x (774 K), T_{eut} (921 K) and T_{liq} (1102 K) mark the onset temperatures of the glass transition, crystallization event, melting peak and liquid state, respectively.

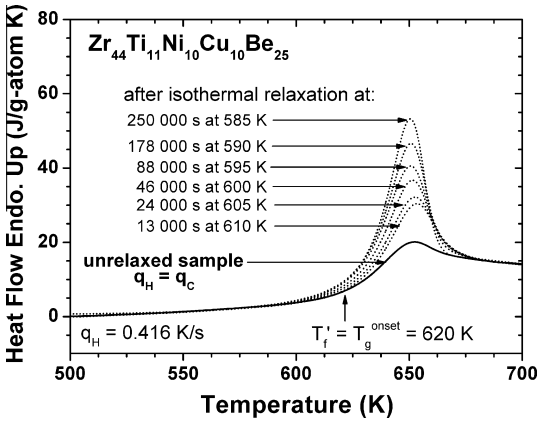

Fig. 2. Enthalpy recovery curves (dotted lines) after isothermal relaxation into the equilibrium liquid at the specified temperatures. The solid line represents the curve of an unrelaxed sample, i.e. heated at the same rate q_H as an immediately preceding cooling q_C from the supercooled liquid region. T_f' is the limiting fictive temperature and approximates T_g^{onset} when $q_H = q_C$.

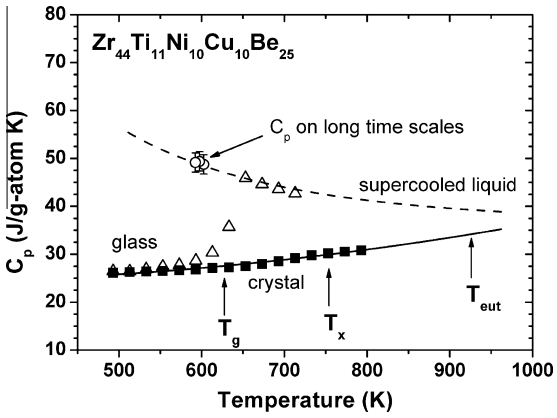

Fig. 3. Measured specific heat capacities C_p of the amorphous (triangles) and crystalline (squares) states of a sample of $Zr_{44}Ti_{11}Ni_{10}Cu_{10}Be_{25}$. The equilibrium liquid on long time scales was reached through isothermal annealing and the C_p estimated from enthalpy recovery experiments (circles). The dotted and solid lines are fits of the experimental data to Eqs. (10) and (11), respectively.

mates the limiting fictive temperature [35]. The recovered enthalpy ΔH_r after heating across the glass transition was calculated as the area between the respective recovery curve and that of the unrelaxed sample at a heating rate of $q_H = 0.416$ K s^{-1}:

$$\Delta H_r = \int_{500\,\mathrm{K}}^{700\,\mathrm{K}} \left[\left(\frac{dQ}{dt}\right)_a - \left(\frac{dQ}{dt}\right)_u \right] A\, dT \tag{9}$$

where $(dQ/dt)_a$ and $(dQ/dt)_u$ are the DSC heat flow signals of the annealed and unrelaxed samples, respectively, in units of mW. Using the constant $A = \mu m^{-1} q_H^{-1}$, where μ is the gram atomic mass of the sample and m is the sample mass in mg, the value of ΔH_r is determined in units of J g atom^{-1}. At 700 K all samples are equilibrated in the metastable supercooled liquid region.

The experimentally determined values of the specific heat capacity as a function of temperature C_p, for the amorphous and crystalline states of the $Zr_{44}Ti_{11}Ni_{10}Cu_{10}Be_{25}$ alloy are shown in Fig. 3. The specific heat capacity values of the glassy state (triangles), the supercooled liquid (triangles) and the crystalline state (filled squares) are shown. The specific heat capacity as determined for long time scales at temperatures below the calorimetric glass transition (circles) was determined using the method in Busch and Johnson [36]. Here the difference in specific heat capacities of the glassy state $C_p^g(T_i)$ and the equilibrium liquid $C_p^l(T_i)$ at a temperature $T_i = T_1 + (T_2 - T_1)/2$ was approximated as $\Delta C_p^{(l-g)} \approx [\Delta H_r(T_1) \;\; \Delta H_r(T_2)]/(T_2 - T_1)$, where ΔH_r is the enthalpy of recovery measured after annealing at the specified temperature.

The temperature dependence of the heat capacities for the equilibrium liquid and crystalline states far above the Debye temperature is found through fitting of the experimental data to the two equations according to Kubaschewski et al. [37]:

$$C_p^l(T) = 3R + aT + bT^{-2} \tag{10}$$

$$C_p^x(T) = 3R + cT + dT^2 \tag{11}$$

where R is the gas constant and C_p^l and C_p^x are the specific heat capacities of the liquid and crystalline states, respectively. The fitting constants were determined to be $a = 0.00653$ J g atom^{-1} K^{-2}, $b = 7.09 \times 10^6$ J K g atom^{-1}, $c = -0.00799$ J g atom^{-1} K^{-2} and $d = 1.94 \times 10^{-5}$ J g atom^{-1} K^{-3}. The specific heat capacity of the liquid close to the melting point was approximated by the difference between the experimentally determined heats of fusion and crystallization $\Delta H_f = 9.3$ kJ g atom^{-1} and $\Delta H_x = 7.5$ kJ g atom^{-1}, respectively. The difference between these two quantities represents the value of the area that lies between the specific heat capacity curves of the liquid and crystalline states in the temperature range from the crystallization to the liquidus temperature,

$$\Delta H_f - \Delta H_x = \int_{T_x}^{T_{liq}} \Delta C_p^l - x(T')dT' \tag{12}$$

where T_x is the temperature of the crystallization peak (761 K) as measured by DSC with a heating rate of 0.333 K s^{-1} and T_{liq} is the liquidus temperature where the sample is completely molten and the Gibbs free energy of the liquid and crystal states are equal (1102 K).

The difference in enthalpy between the liquid and crystalline states can be expressed by integrating the difference in specific heat capacities of the liquid and crystalline states (Eqs. (10) and (11)) and offsetting with the experimentally determined heat of fusion ΔH_f

$$H^{l-x}(T) = \Delta H_f + \int_{T_{liq}}^{T} \Delta C_p^{l-x}(T')dT' \tag{13}$$

In Fig. 4a the enthalpy difference between the liquid and crystalline states of $Zr_{44}Ti_{11}Ni_{10}Cu_{10}Be_{25}$ is plotted as a function of temperature calculated using Eq. (13). The

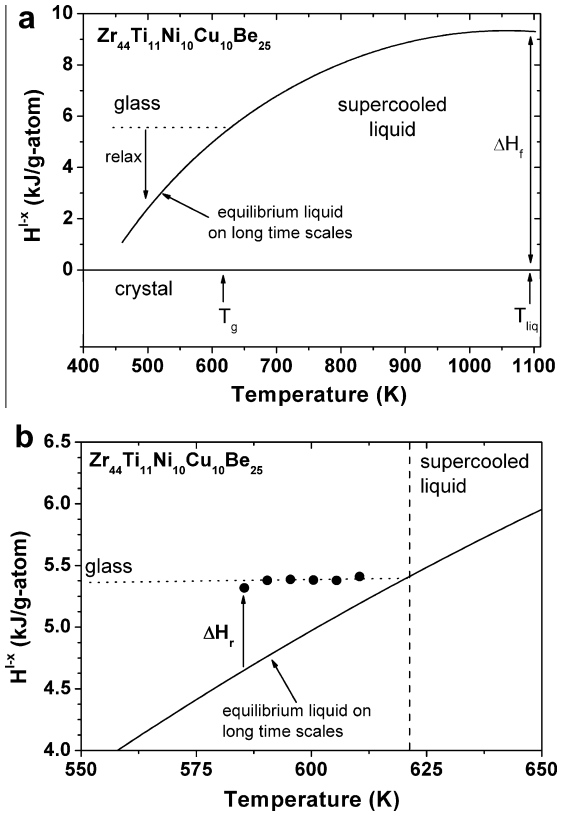

Fig. 4. (a) Calculated enthalpy difference H^{l-x} between the liquid and crystalline states. The experimentally determined heat of fusion $\Delta H_f = 9.3$ kJ g atom^{-1}. T_{liq} was measured to be 1102 K. The glassy state is shown schematically by the dotted line beginning at T_g. The downward arrow schematically indicates the pathway of relaxation. (b) The experimentally determined enthalpy recoveries (filled circles) are plotted above (arrow) the equilibrium curve (solid line). In doing so, the original enthalpic state of the glass prior to relaxation is determined for each annealing temperature.

glassy state is shown schematically as a dotted horizontal line where the residual enthalpy from the supercooled liquid is "frozen in" as the liquid vitrifies into a glass at T_g. The isothermal pathway of enthalpy relaxation from the glassy state into the equilibrium liquid is indicated schematically by the downward arrow. Fig. 4b shows a magnification of the glassy region where the experimentally determined enthalpies of recovery ΔH_r, calculated from the heat flow curves of the completely relaxed samples in Fig. 2, are plotted up from the equilibrium liquid line for each annealing temperature (filled circles).

In Fig. 5 the values of ΔH_r calculated using Eq. (9) are shown for various annealing times at the selected temperatures. For a given annealing temperature the enthalpy recovery as a function of time $\Delta H_r(t)$ approaches a constant value as the sample relaxes into equilibrium at longer annealing times. Relaxation processes in amorphous materials are usually found to be best described by a Kohlrausch–Williams–Watts (KWW) stretched exponential function [38–41] of the form

$$\phi(t) = \phi_{eq}(1 - exp(-(t/\tau)^{\beta_{KWW}}) \quad (14)$$

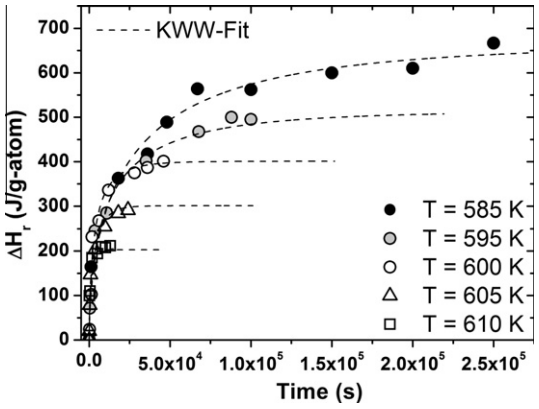

Fig. 5. Experimentally determined enthalpies of recovery ΔH_r after isothermal annealing of the $Zr_{44}Ti_{11}Ni_{10}Cu_{10}Be_{25}$ BMG at various times for the temperatures shown. The dashed lines represent the fits of the KWW equation to the experimental data. The error is of the order of the symbol size.

where $\phi(t)$ is the relaxing quantity and ϕ_{eq} is the value of the relaxing quantity at equilibrium in the supercooled liquid as $t \to \infty$. Here, t is the time, τ is a characteristic relaxation time and β_{KWW} is the stretching exponent parameter ($0 < \beta_{KWW} < 1$). Fitting of the experimental data to the function in Eq. (14) was carried out using a χ^2 minimization algorithm, and the results are shown by the dashed lines in Fig. 5.

Fig. 6 shows the relative change in length $\Delta L/L_o(t)$ of the amorphous samples as they are relaxed from the glassy state into the equilibrium liquid region during isothermal annealing at the temperatures indicated. It can be seen that at lower temperatures the relative changes in length are greater than at higher temperatures closer to the glass transition. The experimental data in Fig. 6 (open circles) are fitted by a KWW function of the form in Eq. (14).

If no temperature changes occur during relaxation conventional thermal expansion effects can be discounted and

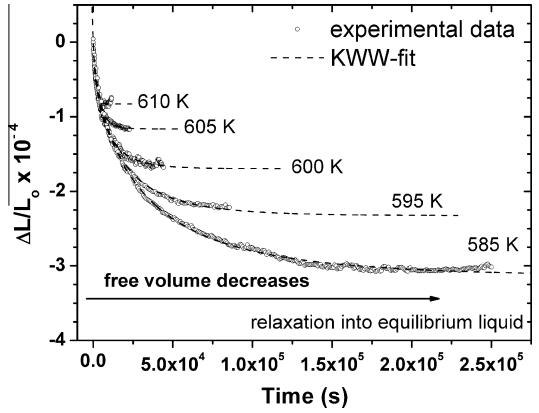

Fig. 6. Experimental relative changes in length $\Delta L/L_o$ of amorphous samples of $Zr_{44}Ti_{11}Ni_{10}Cu_{10}Be_{25}$ during relaxation to the equilibrium liquid for the annealing temperatures shown (open circles). The fits of the experimental data to the stretched exponential (KWW) function are also shown (dashed lines).

the measured reduction in volume is attributed solely to the reduction in excess free volume of the glass. Furthermore, assuming that structural relaxation occurs isotropically, the relative change in free volume of the amorphous sample $\Delta v_f/v_m$ is given by the relative change in length $\Delta L/L_o$ [42–44]:

$$\frac{\Delta v_f}{v_m} = 3\frac{\Delta L}{L_o} \tag{15}$$

The equilibrium viscosities of the $Zr_{44}Ti_{11}Ni_{10}Cu_{10}Be_{25}$ alloy were determined in independent measurements in the vicinity of the glass transition using the three-point beam bending method described in Section 2. Fig. 7 shows the experimental isothermal data for three selected temperatures: 585, 595 and 605 K. All samples were heated to their respective annealing temperatures at a rate of 0.416 K s^{-1} and held there until equilibrium was reached. Fits of Eq. (14) to the measured viscosity data at selected temperatures are shown as dashed lines in Fig. 7. In this equation ϕ_{eq} is taken to be the equilibrium viscosity $\eta_{eq} = \eta_{gl} + \Delta\eta$, where η_{gl} is the initial viscosity of the glassy alloy before relaxation and $\Delta\eta$ is the viscosity increase during relaxation from the glassy state into the equilibrium liquid. η_{eq} therefore corresponds to the constant viscosity value reached by the KWW fits at long times.

The equilibrium viscosity data (open circles) are shown in Fig. 8 along with the viscosities of the glassy alloy immediately before relaxation (shaded circles). A non-linear fit of the VFT equation (Eq. (1)) was performed for the equilibrium data (solid line), giving the fragility parameter $D^* = 25.4$ and the VFT temperature $T_0 = 366.6$ K. Additionally, a fit of the Doolittle equation (Eq. (2)) incorporating the expression for the free volume according to Cohen and Grest (Eq. (4)) was performed (dashed line), giving the fit parameters $bv_m\zeta_0/k = 5000.6$ K, $T_q = 666.6$ K and $4v_a\zeta_0/k = 160.7$ K. Finally, a fit of the equilibrium viscosity data to the Adam–Gibbs equation (Eq. (5)) is also shown (dotted line), resulting in the fit parameters $C = 320.17$ kJ g atom^{-1} and $S_c(T_m^*) = 18.27$ J g atom^{-1} K^{-1}.

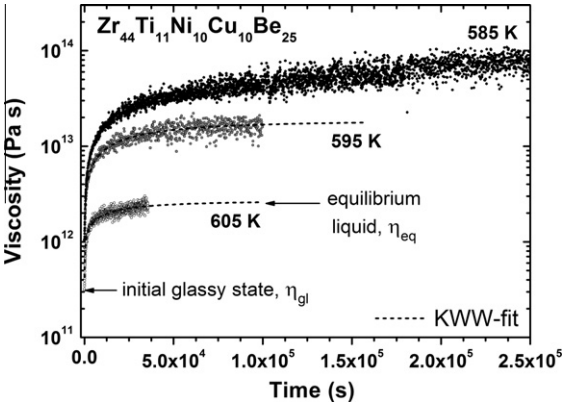

Fig. 7. Isothermal viscosity measurements on $Zr_{44}Ti_{11}Ni_{10}Cu_{10}Be_{25}$ at three selected temperatures below T_g (585, 595 and 605 K). The relaxation from the initial glassy state to the equilibrium liquid is fitted with the stretched exponential (KWW) equation (dashed lines).

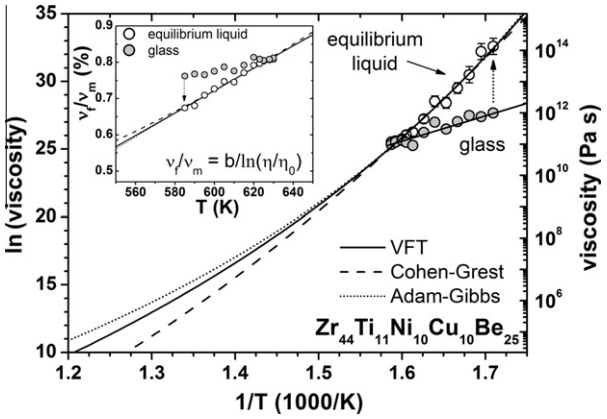

Fig. 8. Equilibrium viscosities (open circles), as well as the viscosities of the glass immediately prior to relaxation (shaded circles), as a function of inverse temperature for the $Zr_{44}Ti_{11}Ni_{10}Cu_{10}Be_{25}$ alloy. The fits to the experimental data using Eq. (2) are shown as the solid, dashed and dotted lines, incorporating the expression for the relative free volume given in Eqs. (3), (4), and (7), respectively. Using Eq. (2) (inset) the relative free volumes are determined from the experimental viscosity data for the equilibrium and glassy states (inset, open and shaded circles, respectively). The curves shown in the inset are the relative free volumes calculated from the fits shown in the main figure. The dotted arrows schematically show the path of relaxation into a more viscous amorphous state with a lower free volume.

The relative free volume v_f/v_m as a function of temperature was calculated using Eqs. (3), (4), and (7) and is shown from 550 to 650 K in the inset to Fig. 8. The relative free volumes of the equilibrium liquid and glassy states were calculated from the experimental viscosity data using Eq. (2) and are shown in the inset (open and shaded circles, respectively). The Doolittle parameter b was determined to be 0.288, using the relation $\alpha_f = b/(D^*T_0)$, where α_{glass} was here measured as 2.22×10^{-5} K^{-1} using a dilatometric method and the value of α_{liq} was taken to be the same as that for Vitreloy 1™ from Ohsaka et al. [45].

4. Discussion

4.1. The kinetics of structural relaxation below T_g

The structural relaxation of the $Zr_{44}Ti_{11}Ni_{10}Cu_{10}Be_{25}$ BMG below the glass transition temperature is quantified here, in part by enthalpy recovery measured upon reheating after isothermally annealing the samples at the selected temperatures. By measuring the exothermic heat flow as a function of time directly during relaxation during DSC Gallino et al. [34] showed that the amount of enthalpy relaxed during the annealing process is equal to the amount recovered upon subsequent reheating. We are thus able to determine the initial enthalpic state of the glassy sample at a certain temperature by calculating the enthalpy of recovery ΔH_r for that temperature, after complete relaxation into the equilibrium liquid, from the respective heat flow curve in Fig. 2 and plotting this value in the positive (endothermic) ΔH direction starting from the H^{1-x} equilibrium curve in Fig. 4b. Furthermore, in Fig. 5 we show the values

of ΔH_r for each annealing temperature determined after various increasingly longer annealing times. The data show a clear saturation of ΔH_r, and approach a constant value as the sample reaches the completely relaxed (equilibrium) state.

Structural relaxation is also quantified here by direct measurement of the change in length of an amorphous sample during annealing (see Fig. 6). Using Eq. (15) these changes in length can be seen as being representative of a total volumetric change due to the reduction in excess free volume of the glass. The experimental data in Fig. 6 show very little changes in length after long annealing times. Additional optical inspection of the loading surface of the amorphous dilatometer samples after relaxation using interference contrast microscopy revealed no indentations from the TMA loading probe, giving no further evidence that viscous flow due to shearing of the sample was present. These results indicate that the glass sufficiently relaxes into the equilibrium liquid on long time scales and that the changes in length during relaxation are solely due to structural changes in the amorphous sample. The fits to the experimental data using Eq. (14) are shown as dashed lines in Fig. 6.

Isothermal measurements of the viscosity of an initially glassy sample at temperatures near the glass transition show that this alloy, if given sufficient time, will completely relax into the metastable equilibrium liquid (see Fig. 7). The viscosity of the glass as a function of time rises sharply from its initial state and steadily approaches a constant value for long times, as seen by the fits of Eq. (14) to the experimental data in Fig. 7. This directly reflects the reduction in the excess free volume in the glass, resulting in a denser amorphous state (see, for example, Fig. 8). No drastic changes in the viscosity are recorded for longer times, indicating that phase separation and/or primary crystallization have not occurred during annealing of this alloy. This is in contrast to the Vitreloy 1™ [46] and Zr–Cu–Ni–Al–Nb [47] BMGs, where clear deviations from stretched exponential relaxation indicate the presence of compositional changes during annealing of the glass.

The data shown in Fig. 9 correspond to the characteristic relaxation times τ and the β_{KWW} values (inset) obtained from fitting Eq. (14) to the experimental data in Figs. 5–7. In Fig. 9 there is very good agreement between the values of τ determined at each annealing temperature for each set of data: the change in viscosity $\Delta\eta$ (filled circles), change in relative length $\Delta L/L_o$ (open circles) and enthalpy recovery ΔH_r (shaded circles). This gives a direct link between each of the relaxing quantities and shows that the volumetric changes observed here during structural relaxation (Fig. 6) can be attributed to the changes in free volume (Figs. 7 and 8).

Furthermore, it can be seen from these results that there is a strong temperature dependence for both τ and β_{KWW}. At lower annealing temperatures the characteristic time for relaxation increases, while the value of β_{KWW} decreases (inset to Fig. 9). As the annealing temperature approaches

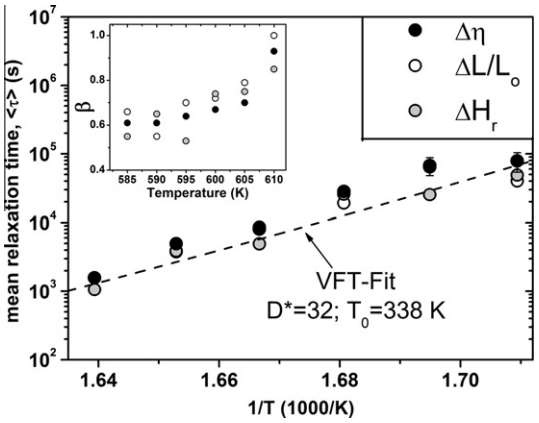

Fig. 9. Mean characteristic relaxation times $\langle\tau\rangle$ obtained from fitting Eq. (14) to the experimental data taken at various annealing temperatures below the glass transition. The relaxation times taken from fitting the change in viscosity $\Delta\eta$ (filled circles), change in relative length $\Delta L/L_o$ (open circles) and enthalpy recovery ΔH_r (shaded circles) are shown. The error is of the order of the symbol size, unless stated otherwise. A fit of the VFT equation (dashed line) to the experimental data is also shown, corresponding to the parameters $D^* = 32$ and $T_0 = 338$ K. The stretching exponent parameter β_{KWW} reaches unity in the proximity of the glass transition (inset).

the glass transition the values of β_{KWW} approach unity, indicating the presence of a purely exponential relaxation. The non-exponential behavior of the measured relaxations is clearly observed at lower annealing temperatures, suggesting a broader distribution of relaxation times. Similar non-exponential behavior was reported recently by Haruyama et al. for the quaternary $Zr_{55}Cu_{30}Ni_5Al_{10}$ BMG in volume relaxation experiments [18] and by Gallino et al. [34] and Zhang and Hahn [31] in enthalpy relaxation experiments on $Zr_{58.5}Cu_{15.6}Ni_{12.8}Al_{10.3}Nb_{2.8}$ and $Zr_{45}Cu_{39.3}Al_{7.0}Ag_{8.7}$ BMGs, respectively.

At this point the significance of the characteristic relaxation time τ obtained from fitting Eq. (14) should be discussed. Here the mean relaxation time $\langle\tau\rangle$ is defined as $\langle\tau\rangle = \tau\beta_{KWW}^{-1}\Gamma(\beta_{KWW}^{-1})$, where Γ is the gamma function. For cases where β_{KWW} is close to unity $\langle\tau\rangle$ and τ are approximately equal. For smaller values of β_{KWW} $\langle\tau\rangle$ becomes greater than τ, reflecting the wider distribution of relaxation times present in the system. Therefore, the use of $\langle\tau\rangle$ is more appropriate when comparing values of τ that have different β_{KWW} values.

The temperature dependence of the mean relaxation times shown in Fig. 9 was investigated with an Arrhenius-like dependence of the form $\langle\tau\rangle = \tau_0\exp(Q/RT)$, where τ_0 is the theoretical infinite temperature limit of the relaxation time and Q is an activation energy. The results of an Arrhenius fit to these data give an apparent activation energy of around 4 eV and a value of $\tau_0 \approx 10^{-32}$ s. This value of τ_0 is unrealistically small, as τ_0 should here be $\sim 10^{-14}$ s, i.e. close to the inverse Debye frequency. Instead, a VFT equation similar to Eq. (1), $\langle\tau\rangle = \tau_0\exp\{D^*T_0/(T - T_0)\}$, with a value of τ_0 set at 10^{-14} s was used to fit the experimental data and is shown as the dotted line in

Fig. 9. The VFT equation provides a good fit to these data with the parameters $D^* = 32$ and $T_0 = 338$ K. This result is similar to that obtained from the volumetric relaxation times reported in Haruyama et al. [18] for a $Zr_{55}Cu_{30}Ni_5Al_{10}$ BMG.

The applicability of the VFT equation here shows that these relaxation times reflect, to some degree, the VFT behavior of the equilibrium undercooled liquid itself. As the temperature is lowered from T_g the time needed for complete relaxation into the equilibrium liquid increases (Fig. 9). Intuitively, if the viscosity of the undercooled liquid approaches infinity at a certain temperature then so should the characteristic structural relaxation time (τ or $\langle\tau\rangle$). Therefore, the structural relaxation time should have roughly the same temperature dependence as that of the equilibrium liquid itself. In fact, this seems to be the case here, as the VFT parameters obtained from the equilibrium viscosity data (Fig. 8) are in good agreement with those obtained from the Kohlrausch relaxation times (Fig. 9).

4.2. Enthalpy and free volume

The reduction in enthalpy of the glass during annealing can be understood as a result of the reduction in the excess free volume that was present during formation of the glass while cooling from the supercooled liquid. In other words, the annealing out of the free volume of a glass is associated with a corresponding release of heat, resulting in an overall lower enthalpic state. Van den Beukel and Sietsma [24] assumed a linear relationship of the form

$$\Delta H = \beta' \left(\frac{\Delta v_f}{v_m} \right) \tag{16}$$

where ΔH is the change in enthalpy due to the change in relative free volume $\Delta v_f/v_m$. v_m is taken here as the atomic volume at the liquidus temperature, 1.67×10^{-29} m^3, and was previously determined for another BMG alloy with a very similar composition $Zr_{41.2}Ti_{13.8}Ni_{12.5}Cu_{10}Be_{22.5}$ (Vitreloy 1™) [45]. The proportionality constant β' therefore has the same units of enthalpy, i.e. kJ g atom^{-1}.

A linear relationship is found between the amount of enthalpy recovered using DSC, ΔH_r, and the decrease in excess free volume from the glassy state using volumetric relaxation, $\Delta(v_f/v_m)_{glass}$, for each annealing temperature, and is shown in Fig. 10. The constant β' from Eq. (16) is determined here to be 622.7 ± 20 kJ g atom^{-1}. This result is in good agreement with similar studies performed on a quaternary $Zr_{55}Cu_{30}Al_{10}Ni_5$ BMG using direct density measurements to quantify the free volume change. Slipenyuk and Eckert [16] reported a value of $\beta' = 552 \pm 15$ kJ g atom^{-1} and Haruyama et al. [18] report a value of 718.2 kJ g atom^{-1} for the above alloy. It has been suggested that β' represents the formation enthalpy of an amount of free volume with the magnitude of one atomic volume [24], which has been determined in these studies to be two or three times greater than the formation enthalpy of a vacancy in a pure Zr crystal lattice [48].

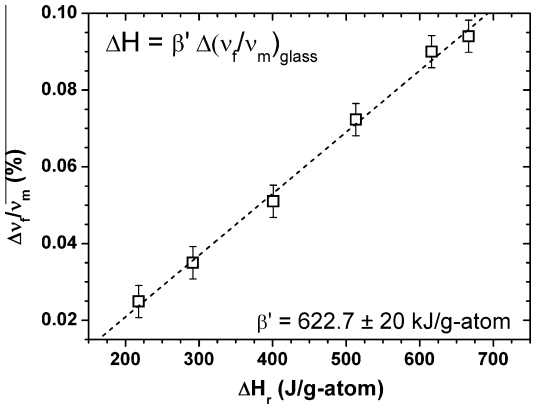

Fig. 10. The experimentally determined values $\Delta(v_f/v_m)_{glass}$ vs. ΔH_r are shown for each annealing temperature (open squares) along with a linear fit to the data (dashed line). The proportionality constant β' was found to be 622.7 ± 20 kJ g atom^{-1}.

The linearity between ΔH_r and $\Delta(v_f/v_m)_{glass}$ suggests a similar relationship between the equilibrium curves for enthalpy and relative free volume, i.e. H^{1-x} and v_f/v_m, respectively. Indeed, by matching these curves, as shown in Fig. 11, it can be seen that all three models of v_f/v_m agree very well with the H^{1-x} curve in the vicinity of the glass transition (see Fig. 13). In this temperature range the free volume and enthalpy curves appear to be linear. Within this linear regime we can estimate the value of β' for the equilibrium liquid as $\beta'_{eq} \approx \Delta H^{1-x}/\Delta(v_f/v_m)$, where $\Delta H^{1-x} = H^{1-x}(T_1) - H^{1-x}(T_2)$ and $\Delta(v_f/v_m) = v_f(T_1)/v_m - v_f(T_2)/v_m$ and T_1 and T_2 mark the temperature range in which H^{1-x} and v_f/v_m behave linearly (550–650 K). We calculate the value of β'_{eq} to be ~680 kJ g atom^{-1}, which

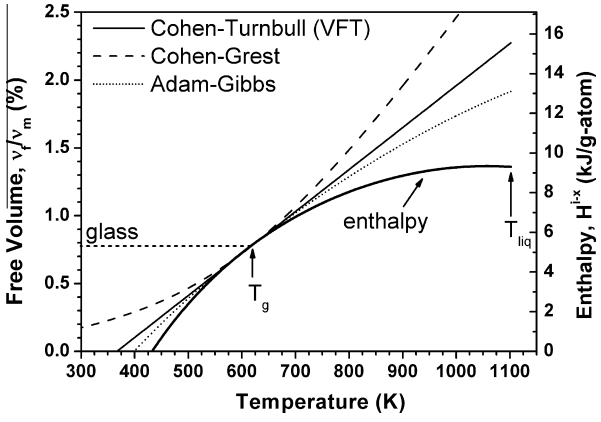

Fig. 11. Relative free volume curves of the equilibrium liquid of $Zr_{44}Ti_{11}Ni_{10}Cu_{10}Be_{25}$ according to the Cohen–Turnbull, Cohen–Grest and Adam–Gibbs (solid, dashed and dotted lines, respectively) models. The thick, solid line is the enthalpy difference between the liquid and crystalline states H^{1-x}, calculated from the C_p^{l-x} curve and the experimentally determined value of ΔH_f. The glassy state is shown schematically by the heavy dotted line.

is in agreement with the value of β' calculated in the glassy state (622.7 ± 20 kJ g atom^{-1}).

The high value of β'_{eq} reported here corresponds to the enthalpy necessary for the formation of an amount of free volume in the equilibrium liquid equal to v_m. However, flow processes in liquids usually require critical volumes that are only a fraction of v_m. Indeed, Cohen and Turnbull reported a value for the critical volume of around $0.8v_m$ for Van der Waals liquids and closer to $0.1v_m$ for pure metals [8]. In the light of this, we find our calculated b value of 0.288 for this alloy (see Eq. (2)) in its undercooled state to be physically acceptable. Furthermore, if we choose instead to use the reduced free volume $x = v_f/(bv_m)$, thus taking into account only the critical volume necessary for flow, we arrive at a reduced enthalpy of formation for the free volume $\beta_{eq} \approx \Delta H^{1-x}/\Delta x$ of $\sim$200 kJ g atom^{-1} for the deeply undercooled equilibrium liquid from 550 to 650 K. Supposing now that the same critical amount of free volume is required for structural relaxation in the glass below T_g, we calculate a reduced enthalpy of formation of $\beta \approx 180$ kJ g atom^{-1} for the glass.

In Eq. (16) it is assumed that the enthalpy of formation for the free volume remains constant with temperature. In the glassy state of this alloy the enthalpy of formation for the free volume determined from structural relaxation experiments is indeed constant over the temperature range investigated (Fig. 10). In the equilibrium liquid, however, this formation enthalpy can be approximated as a constant only in those temperature ranges where the enthalpy and free volume functions of the equilibrium liquid behave linearly, e.g. in the glass transition region in Fig. 11, i.e. the slope of the enthalpy curve with respect to the slopes of the free volume curves remains constant throughout a given temperature range in the equilibrium liquid. In order to analyze the exact behavior of the free volume formation enthalpy over the entire temperature range of the equilibrium liquid it is necessary to determine the instantaneous change in the slopes of the enthalpy and free volume functions.

In Fig. 12 we calculate the reduced enthalpy of free volume formation as the change in $H^{1-x}(T)$ with respect to the change in the reduced free volume $x(T)$ or $\beta_{eq} = dH^{1-x}/dx$. Fig. 12 shows the calculated values of β_{eq} for each of the free volume models considered here in the temperature range from the VFT temperature T_0 to the melting temperature T_{eut}. The experimental equilibrium viscosity data were taken in the vicinity of T_g and used in each free volume model; as such, the intersection of these curves at T_g is a result of that fact. In each model for β_{eq} shown in Fig. 12 the value increases as the temperature decreases from T_{eut} to T_0. This is primarily a reflection of the increasing slope of the H^{1-x} curve as the liquid is undercooled below its melting point (i.e. the C_p^l curve in Fig. 3). According to these estimations the reduced enthalpy of free volume formation in the equilibrium liquid increases from about 100 kJ g atom^{-1} ($\sim$1 eV) at the melting point to about 200 kJ g atom^{-1} ($\sim$2 eV) around T_g.

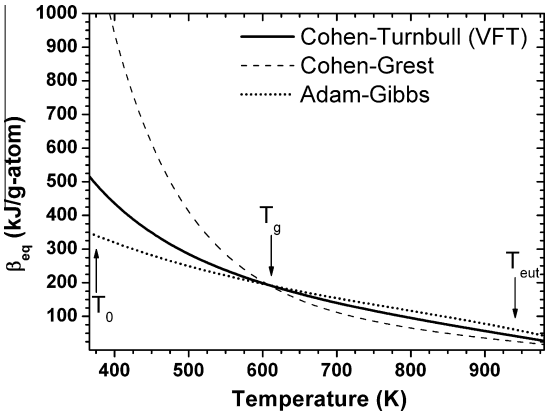

Fig. 12. Reduced free volume formation enthalpy β_{eq}, calculated using $\beta_{eq} = dH^{1-x}/dx$, where $x(T)$ is the reduced free volume of the equilibrium liquid according to the free volume models given in Eqs. (3), (4), and (7). The solid, dashed and dotted lines represent β_{eq} calculated according to each free volume model. The temperatures indicated are the VFT temperature T_0, the glass transition temperature T_g and the melting temperature T_{eut}.

Of the free volume curves shown in Fig. 11 the Cohen and Grest model (dashed line) is the only one that has an appreciable change in the slope over the entire temperature range. Below T_g the slope of the free volume curve of the equilibrium liquid in the Cohen and Grest interpretation decreases steadily. Mathematically, this is the result of the requirement that in the Cohen and Grest model $v_f > 0$ for all $T > 0$. This leads to an apparent, and intuitively unphysical, divergence in β_{eq} for very low temperatures (dashed line, Fig. 12). As the other two models of the free volume presented show no or very little change in the slope over the temperature range considered it can be deduced that the increase in β_{eq} with decreasing temperature is due primarily to the increase in the specific heat capacity of the liquid during undercooling.

At low temperatures the free volume of the equilibrium liquid according to the model of Cohen and Turnbull (Eq. (3)) vanishes at $T_0 = 366.6$ K, while in the model proposed by Cohen and Grest (Eq. (4)) the free volume decreases to 0 only at $T = 0$, as discussed in the previous paragraph. In the Adam–Gibbs model for the equilibrium free volume the equations for viscous flow (Eqs. (5) and (7)) v_f/v_m vanish for this alloy at a temperature of $T_0^* = 400$ K, where T_0^* is defined as in Gallino et al. [14] as the temperature at which the configurational entropy $S_c(T)$ vanishes in the Adam–Gibbs fit of the equilibrium viscosity data. The similarity between T_0 and T_0^* suggests the existence of a state in the equilibrium liquid at $T \neq 0$ with a single possible configuration, i.e. an ideal packing state, where the barriers with respect to viscous flow become infinitely large. Additionally, we report in Section 3 a value of C for this alloy of 320.17 kJ g atom^{-1} and find that this value is in very good agreement with the thermodynamic fragility analysis performed in Gallino et al. [14], i.e. for Zr-based BMG systems C compares well with the activation energy for diffusion of larger atomic species measured around

the glass transition (~300 kJ g atom^{-1} [49]), indicating their crucial involvement in the cooperative rearrangements necessary for flow and structural relaxation.

In Fig. 13 the different models of the relative free volume are shown in the vicinity of the glass transition along with the equilibrium curve of the enthalpy H^{1-x}. The experimental enthalpy recovery data ΔH_r are reproduced from Fig. 4b (filled circles). Calculated from the viscosity data in Fig. 8, the relative free volumes in the equilibrium liquid $(v_f/v_m)_{eq}$ are shown (open circles), as well as the excess free volume of the glass $(v_f/v_m)_{glass}$ (shaded circles). Additionally, the reduction in excess free volume of the glass $\Delta(v_f/v_m)_{glass}$, determined directly from the volumetric relaxation experiments using Eq. (15), are shown (open squares) with reference to the equilibrium v_f/v_m curves. The free volume changes reported here during isothermal relaxation are of the order of 0.05%. When compared with similar research in other BMG systems, where the reported excess free volume reduction ranges from 0.04% to 0.10% (see, for example, Slipenyuk and Eckert [16], Haruyama and Inoue [17] and Haruyama et al. [18]), we find good agreement with our experimental results.

It has to be emphasized that each data set representing $(v_f/v_m)_{glass}$ depicted in Fig. 13, as well as ΔH_r, was obtained in independent measurements on the glassy samples. Additionally, we find remarkable agreement between the values of $(v_f/v_m)_{glass}$ taken from volumetric relaxation and those calculated from viscosity measurements. This is an indication that the change in viscosity during relaxation into the equilibrium liquid directly reflects the change in free volume, as well as in enthalpy.

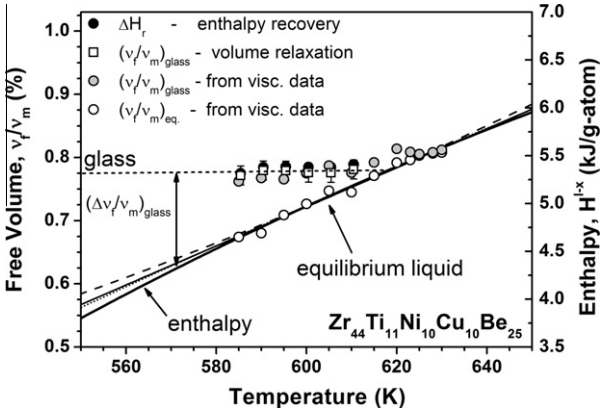

Fig. 13. Enthalpy recoveries ΔH_r (dark circles) and excess free volume of the glass $(v_f/v_m)_{glass}$ (open squares) calculated from the changes in length during relaxation into the equilibrium liquid. The relative free volumes of the initial glassy and equilibrium states are calculated from the experimental viscosity data using Eq. (2) and are shown as shaded and open circles, respectively. The relative free volume curves of the equilibrium liquid shown in Fig. 11 are reproduced here, as well as the calculated enthalpy difference between the liquid and crystalline states as a function of temperature. The glassy state is schematically indicated with the heavy dotted line. $(\Delta v_f/v_m)_{glass}$ is the excess free volume frozen into the glassy state.

4.3. Free volume of Vitreloy 1™

To investigate the predictive ability of each free volume model for a higher temperature range, i.e. above the melting temperature, we revisit the case of free volume and viscous flow for Vitreloy 1™ as reported in Masuhr et al. [9]. Equilibrium viscosity studies in the vicinity of the glass transition using a three-point beam bending method have been performed on this particular composition [39], as well as rotating cup viscometry at temperatures in the liquid state [50]. In Fig. 14 the relative free volume curves for the Vitreloy 1™ alloy are shown as a function of temperature, along with the experimental viscosity data taken from Busch et al. [39] and Way et al. [50] expressed as relative free volume, in the vicinity of the glass transition (open circles) and above T_{eut} (open squares). It should be noted that Way et al. [50] reported a strong to fragile transition for this alloy for temperatures above 1225 K, we therefore only examine viscosity data representing the liquid state before this transition, i.e. data that represent only the kinetically strong state.

In this work only the low temperature viscosity data taken from three-point beam bending experiments were considered during fitting and used to construct the relative free volume curves, similarly to Fig. 11. Considering only the low temperature data the fit parameters from Eqs. (2) and (4) were determined to be $bv_m\varsigma_0/k = 7675.4$ K, $T_q = 453.6$ K and $4v_a\varsigma_0/k = 59.9$ K, with the parameter b calculated as 0.164. Non-linear fitting of Eqs. (1) and (5) has already been performed for this alloy by Gallino et al. [14], and the parameters D^*, T_0, C and $S_c(T_m^*)$ were determined to be 22.0, 387 K, 295.11 kJ g atom^{-1} and 19.07 J g atom^{-1} K^{-1}, respectively. The relative free volume curves calculated using the Cohen–Turnbull, Cohen–Grest and Adam–Gibbs models are shown as the solid, dashed and dotted lines in Fig. 14, respectively.

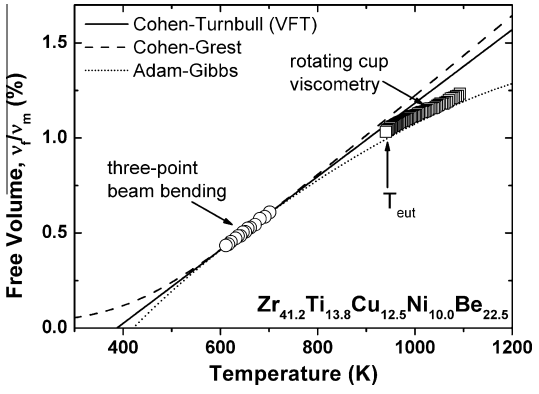

Fig. 14. Relative free volumes of the $Zr_{41.2}Ti_{13.8}Cu_{12.5}Ni_{10.0}Be_{22.5}$ BMG calculated from experimental viscosity data taken in the vicinity of the glass transition (open circles) [39] and in the liquidus region (open squares) [50]. Fits of the Cohen–Turnbull (solid line), Cohen–Grest (dashed line) and Adam–Gibbs (dotted line) free volume models are shown considering only the low temperature data (open circles).

The Adam–Gibbs model of the relative free volume (dotted line) from Eq. (7) shows good agreement with the experimental data corresponding to the liquid state at high temperatures (open squares), even though these data were not considered for fitting. The low free volume at temperatures above the melting point is directly related to the high melt viscosity of this alloy (~100 Pa s), which is thought to be due to pronounced short- and medium-range order in the liquid [50]. The good predictive ability of the Adam–Gibbs model in this case lies in its dependence on the configurational entropy, which for multi-component BMG alloys shows little change around the melting temperature, due to the aforementioned ordering processes.

5. Summary and conclusions

The reduction in excess free volume $\Delta(v_f/v_m)_{glass}$ and the kinetics of structural relaxation of the $Zr_{44}Ti_{11}Ni_{10}Cu_{10}Be_{25}$ BMG alloy in the glassy state were determined at temperatures below T_g using methods of enthalpy recovery measured by DSC and length relaxation measured in a dilatometer, as well as through measurement of the change in viscosity using a three-point beam bending method in a TMA. It was found that the kinetics of structural relaxation can be well described by a stretched exponential function with β_{KWW} values approaching unity as the glass transition is approached. This is in good accord with similar investigations of the enthalpy and volume relaxation in other Zr-based BMG systems. The isothermal change in length of the amorphous samples during relaxation into the metastable equilibrium liquid was used to directly determine the change in excess free volume of the glass. A linear relationship between ΔH_r and $\Delta(v_f/v_m)_{glass}$ was found in the vicinity of the glass transition and the proportionality constant was determined to be 622.7 ± 20 kJ g atom^{-1}, which has been interpreted as the formation enthalpy for an amount of free volume with the magnitude of one atomic volume. Since flow processes are known to occur when a critical amount of free volume is reached ($\sim 0.1 v_m$ for metallic species), the formation enthalpy necessary for this critical free volume is accordingly lower. According to our results the formation enthalpies for the critical amount of free volume needed for structural relaxation, as well as for viscous flow, are similar, ~180–200 kJ g atom^{-1} near the glass transition. Our analysis also suggests that this formation enthalpy is a function of temperature and increases from ~100 kJ g atom^{-1} near the melting point to ~200 kJ g atom^{-1} around the glass transition temperature.

The values of v_f/v_m in the initially glassy state were calculated from viscosity measurements for a range of annealing temperatures using the Doolittle equation. These values are in good agreement with the independently measured amounts of excess free volume reduction in the glass taken from the dilatometric experiments and presents an extension to the results of our previous work [51]. Furthermore, the excellent agreement of these data with the experimentally determined enthalpy recoveries at the same annealing temperatures shows a very consistent picture of excess free volume reduction as analyzed by each of the techniques reported here.

Using equilibrium viscosity data taken near T_g models of the relative free volume in the equilibrium liquid according to Cohen and Turnbull, Cohen and Grest and Adam and Gibbs were calculated for the temperature range 300–1100 K. Each model provides an excellent fit to the experimental data. The VFT temperature for this alloy T_0 matches well with the temperature (within about 35 K) at which the configurational entropy of the equilibrium liquid vanishes in the Adam–Gibbs fit of the equilibrium viscosity data T_0^*. This suggests a link between the kinetics and thermodynamics of viscous flow.

Examination of high temperature experimental viscosity data for the Vitreloy 1™ BMG alloy revealed that the Adam–Gibbs equation for viscous flow has good ability to predict the free volume of this alloy in the temperature region above the melting point. This supports the validity of the Adam–Gibbs model for multi-component BMG forming melts over a wide temperature range.

Finally, based on the findings presented in this paper we draw the following conclusions.

- Structural relaxation in the $Zr_{44}Ti_{11}Ni_{10}Cu_{10}Be_{25}$ BMG is consistent within the free volume model, as measured by calorimetric and volumetric methods.
- The enthalpy of formation for free volume in the glassy state of this alloy is similar to that of the equilibrium liquid in the vicinity of T_g. In the equilibrium liquid, however, the formation enthalpy does not remain constant and increases with decreasing temperature.
- The Adam–Gibbs model for the equilibrium viscosity not only provides a robust thermodynamic description of the glass transition, but also offers a useful picture of the free volume at temperatures near the melting point.

Acknowledgements

The authors thank Liquidmetal© Technologies for providing the material Vitreloy 1b™. This work was supported by the Deutsche Forschungsgemeinschaft (German Research Foundation).

References

[1] Angell CA. J Non-Cryst Solids 1991;131–133:13.
[2] Angell CA. Science 1995;267:1924.
[3] Vogel H. Phys Z 1921;22:645.
[4] Fulcher G. J Am Ceram Soc 1925;8:339.
[5] Tammann G, Hesse W. Z Anorg Allg Chem 1926;156:245.
[6] Nemilov SV. Glass Phys Chem 1995;21:379.
[7] Doolittle AK. J Appl Phys 1951;22:1471.
[8] Cohen H, Turnbull D. J Chem Phys 1959;31:1164.
[9] Masuhr A, Waniuk TA, Busch R, Johnson WL. Phys Rev Lett 1999;82:2290.

[10] Williams M, Landel R, Ferry D. J Am Chem Soc 1955;77:3701.
[11] Cohen H, Turnbull D. J Chem Phys 1961;34:120.
[12] Grest G, Cohen H. Adv Chem Phys 1981;48:455.
[13] Adam G, Gibbs JH. J Chem Phys 1965;43:139.
[14] Gallino I, Schroers J, Busch R. J Appl Phys 2010;108:063501.
[15] Russew K, Sommer F. J Non-Cryst Solids 2003;319:289.
[16] Slipenyuk A, Eckert J. Scripta Mater 2004;50:39.
[17] Haruyama O, Inoue A. Appl Phys Lett 2006;88:131906.
[18] Haruyama O, Nakayama Y, Wada R, Tokunaga H, Okada J, Ishikawa T, et al. Acta Mater 2010;58:1829.
[19] Kawamura Y, Inoue A. Appl Phys Lett 2000;77:1114.
[20] Wilde G, Görler GP, Willnecker R, Fecht HJ. J Appl Phys 2000;87:1141.
[21] Fan GJ, Fecht HJ. J Chem Phys 2002;116:5002.
[22] Spaepen F. Scripta Mater 2006;54:363.
[23] Nagel C, Rätzke K, Schmidtke E, Wolff J, Geyer U, Faupel F. Phys Rev B 1998;57:224.
[24] van den Beukel A, Sietsma J. Acta Metall Mater 1990;38:383.
[25] Ruitenberg G, De Hey P, Sommer F, Sietsma J. Phys Rev Lett 1997;79:4830.
[26] van den Beukel A, Sietsma J, De Hey P. Acta Metall Mater 1998;46:5873.
[27] Wen P, Wang W, Zhao Y, Zhao D, Pan M, Li F, et al. Phys Rev B 2004;69:8.
[28] Launey M, Busch R, Kruzic J. Scripta Mater 2005;54:483.
[29] Launey M, Kruzic J, Li C, Busch R. Appl Phys Lett 2007;91:051913.
[30] Launey M, Busch R, Kruzic J. Acta Mater 2008;56:500.
[31] Zhang Y, Hahn H. J Non-Cryst Solids 2009;355:2616.
[32] Waniuk T, Schroers J, Johnson W. Phys Rev B 2003;67:184203-1.
[33] Hagy HE. J Am Ceram Soc 1963;46:93.
[34] Gallino I, Shah M, Busch R. Acta Mater 2007;55:1367.
[35] Evenson Z, Gallino I, Busch R. J Appl Phys 2010;107:123529.
[36] Busch, Johnson. Appl Phys Lett 1998;72:2695.
[37] Kubaschewski O, Alcock C, Spencer P. Materials thermochemistry. 6th ed. New York: Pergamon Press; 1993.
[38] Ediger MD, Angell CA, Nagel SR. J Phys Chem 1996;100:13200.
[39] Busch R, Bakke E, Johnson WL. Acta Metall Mater 1998;46:4725.
[40] Vilgis TA. Phys Rev B 1993;47:2882.
[41] Böhmer R, Ngai KL, Angell CA, Plazek DJ. J Chem Phys 1993;99:4201.
[42] Mulder AL, van der Zwaag S, van den Beukel A. Acta Metall Mater 1984;32:1895.
[43] van den Beukel A, Huizer E. Acta Metall Mater 1987;35:2843.
[44] Friedrichs H, Neuhäuser H. J Phys Condens Mater 1989;1:8305.
[45] Ohsaka K, Chung SK, Rhim W, Peker A, Scruggs D, Johnson W. Appl Phys Lett 1997;70:726.
[46] Waniuk TA, Busch R, Masuhr A, Johnson WL. Acta Mater 1998;46(15):5229.
[47] Evenson Z, Raedersdorf S, Gallino I, Busch R. Scripta Mater 2010;63:573.
[48] Bacq OL, Willaime F. Phys Rev B 1999;59:8508.
[49] Faupel F, Werner F, Macht MP, Mehrer H, Naundorf V, Rätzke K, et al. Rev Mod Phys 2003;75:237.
[50] Way C, Wadhwa P, Busch R. Acta Mater 2007;55:2977.
[51] Evenson Z, Busch R. J Alloys Compd 2010, in press. doi:http://dx.doi.org/10.1016/j.jallcom.2010.12.044.